

## Molecular architecture of a galactoglucan from *Rhizobium meliloti*

Rengaswami Chandrasekaran <sup>a,\*</sup>, Eun J. Lee <sup>a</sup>,  
Vadakkanthara G. Thailambal <sup>a</sup>, Ludovicus P.T.M. Zevenhuizen <sup>b</sup>

<sup>a</sup> Whistler Center for Carbohydrate Research, Smith Hall, Purdue University, West Lafayette,  
IN 47907, USA

<sup>b</sup> Department of Microbiology, Agricultural University, Hesselink van Suchtelenweg 4,  
6703 CT Wageningen, Netherlands

(Received December 20th, 1993; accepted in revised form March 15th, 1994)

---

### Abstract

*Rhizobium meliloti* mutants produce a linear, acidic exopolysaccharide with alternating galactopyranosyl and glucopyranosyl units having (1 → 3) linkages. It has a 4,6-*O*-pyruvic cyclic acetal group on the  $\alpha$ -galactosyl and 6-*O*-acetyl ester group on the  $\beta$ -glucosyl units. X-ray diffraction patterns from polycrystalline and well oriented specimens of its potassium salt indicate that the polymer forms a 2-fold helix of pitch 15.89 Å. The three-dimensional structure has been determined and refined by using the X-ray intensities and the linked-atom least-squares technique. The details of the antiparallel packing arrangement of two helices in an orthorhombic unit cell,  $a = 14.49$ ,  $b = 9.79$ , and  $c = 15.89$  Å, reveal that each disaccharide repeating unit is associated with one potassium and three water molecules. The helices are interconnected by a series of  $\cdots \text{COO}^- \cdots \text{K}^+ \cdots \text{W} \cdots \text{COO}^- \cdots$  interactions. Both pyruvyl and acetyl groups, which are on the periphery of the helix, are involved in the association of the polysaccharide chains and thus appear to be an integral component of the galactoglucan in the nodule invasion process.

---

### 1. Introduction

Symbiotic nitrogen fixation is a complex process involving physiological and biochemical properties of both the bacterium and the host plant. The first step in this process involves the selective attachment to and penetration of the plant by

---

\* Corresponding author. Tel., (317) 494-4923; FAX, (317) 494-7953.



proportion of EPS I in the mixture, the viscoelastic properties change abruptly producing a typical weak gel system [14]. Potentiometric and chiro-optical data [15], as a function of the degree of ionization, indicate the absence of a cooperative conformational transition; solution properties [15], as a function of ionic strength and temperature, suggest that EPS II in solution adopts a disordered conformation characterized by moderate flexibility.

Mutants of *Rhizobia* are capable of forming nitrogen-fixing nodules on alfalfa despite the fact that many of them do not produce EPS I. Because they are functionally interchangeable, it is believed that both EPS I and EPS II promote nodule invasion by the same mechanism [16]. The possible structural roles of rhizobial exopolysaccharides in symbiosis include shielding the *Rhizobia* from plant defense responses; participating in the recognition of root hairs that are susceptible to invasion; functioning as carriers of extracellular enzymes; forming part of the matrix of infection threads; and functioning as a signal to the plant, either in a high molecular weight form or as an oligosaccharide [7,17].

Current information does not allow one to distinguish between the above possibilities. However, both EPS I and EPS II have common properties that would allow them to function in all of the possible mechanisms. If the polysaccharides function by a mechanism requiring specific binding and/or recognition, then a knowledge of their three-dimensional structures might provide some insight into the mechanism of their action. Here, we describe the molecular architecture of the potassium salt of EPS II. The atoms within its disaccharide repeating unit are labeled as shown in Fig. 1.

## 2. Experimental

**Fiber preparation.**—An aqueous solution (0.3 mg/mL) of the EPS II polysaccharide [12] was dialyzed against 10 mM KF (4 × 250 mL) at room temperature. Any excess salt was removed by repeated dialysis against distilled water. The

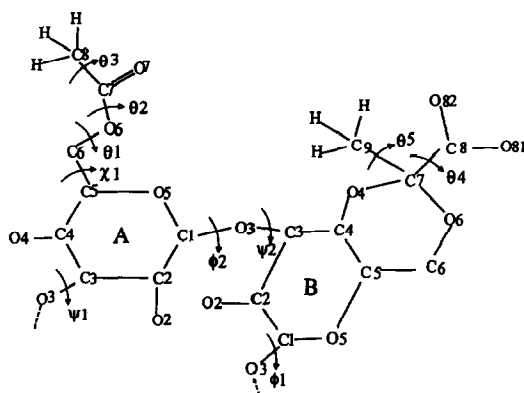


Fig. 1. Schematic representation and atom labeling of a disaccharide repeating unit of the galactoglucon. The major conformation angles are also indicated.

solution of the potassium salt of EPS II was then freeze-dried. A small amount of this material was dissolved in water (2 mg/mL) and well mixed. A few drops of the solution were placed in the gap between the two glass rods in a conventional fiber puller. The solution was allowed to dry slowly under controlled relative humidity of ~43%, and gradually stretched to achieve orientation along the fiber axis. The density of the fiber was measured by the flotation method using a mixture of bromobenzene and bromoform.

*X-ray intensity data.*—Diffraction patterns were recorded on flat photographic films in pinhole cameras using Ni-filtered  $\text{Cu K}\alpha$  radiation ( $\lambda = 1.5418 \text{ \AA}$ ). Typical sample-to-film distance was 35 mm. A steady stream of He gas, after bubbling through the appropriate saturated salt solution, was used to flush the specimen chamber in order to maintain the fiber at the desired relative humidity. Unit cell dimensions were measured using patterns obtained from polycrystalline and oriented fibers dusted with calcite powder (of characteristic spacing  $3.035 \text{ \AA}$ ) for internal calibration.

The diffraction pattern was scanned on an Optronics P-1000 rotating drum microdensitometer with a  $100\text{-}\mu\text{m}$  raster step. Optical density information was stored on magnetic tape on a gray scale of 0–255 in the range of 0–3 OD unit and then transferred to a VAX 8558 computer. The pattern was displayed on a Lexidata 3400 raster graphics system interfaced with the VAX and a data tablet used to locate features on the displayed image. Based on points selected between layer lines, and away from the spots, the background in the film was estimated and subtracted from the entire pattern [18]. Radial and angular profiles of a few sharp Bragg spots in the background corrected pattern were used to determine the disorientation in the specimen and the reflection boundaries. Bragg intensities were calculated by integrating the optical densities inside each spot boundary [19]. Lorentz and polarization corrections were applied before computing the observed structure amplitudes.

*Diffraction pattern and unit cell contents.*—A typical X-ray fiber diffraction pattern from the  $\text{K}^+$  salt of EPS II obtained at 43% relative humidity (Fig. 2) indicates that the specimen is polycrystalline and well oriented. The pattern contains 43 non-meridional and 2 sharp meridional Bragg reflections, extending out to  $2.5 \text{ \AA}$  resolution. The spots can be indexed on the basis of a rectangular lattice with unit cell dimensions (and standard deviations)  $a = 14.49(2)$ ,  $b = 9.79(2)$ , and  $c = 15.89(2) \text{ \AA}$ . Strong meridional spots on the 2nd and 4th layer lines indicate that the polysaccharide forms a two-fold helix of pitch  $15.89 \text{ \AA}$ . Systematic absences of the  $(h00)$ ,  $(0k0)$ , and  $(00l)$  reflections having  $h$ ,  $k$ , and  $l$  odd suggest that the helices are packed in an orthorhombic unit cell consistent with space group  $\text{P2}_12_12_1$ . According to the fiber density ( $1.54 \text{ g/mL}$ ), there could be two helices packed antiparallel to each other, one at the corner and the other at the center, related by  $2_1$  axes parallel to the  $a$ - and  $b$ -axes. Besides, one  $\text{K}^+$  ion and up to three water molecules could be associated with each disaccharide repeating unit.

It is appropriate to mention that a set of 24 below threshold reflections, which are too weak to be seen on the film, was appended to the observed data that was

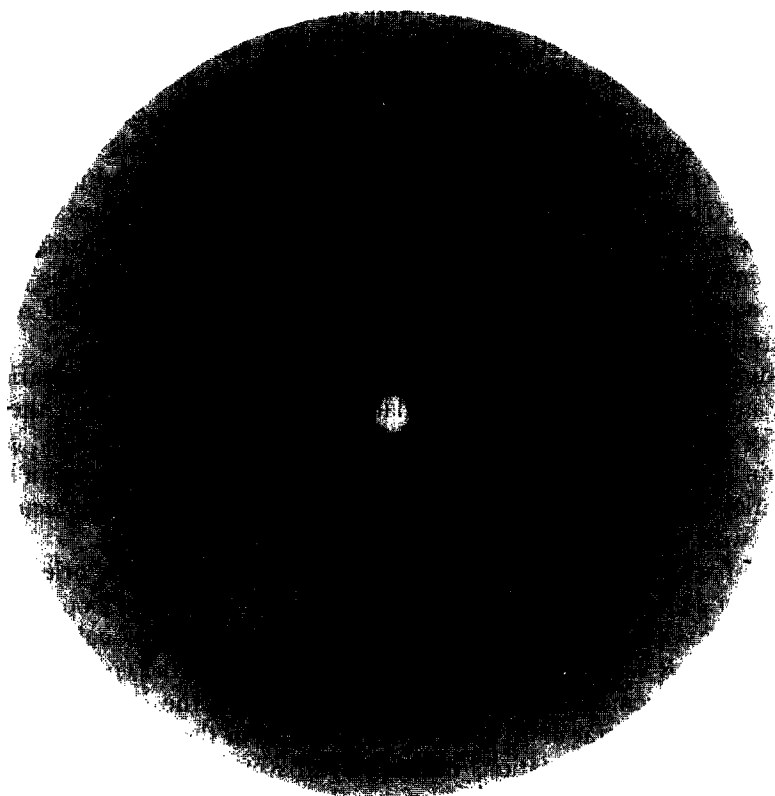


Fig. 2. X-ray diffraction pattern from a well oriented and polycrystalline fiber of the potassium salt of galactoglucan.

used in conducting the structure analysis. The lowest measured intensity was assigned, as the threshold value, to every weak reflection; and it was included in the least-squares refinement only when the calculated structure amplitude was higher than the observed amplitude.

*Model building and refinement.*—Single helix models of EPS II having two-fold screw symmetry and a pitch of 15.89 Å were generated using the linked-atom least-squares program [20]. Pyranose rings were initially assigned the standard  ${}^4C_1$  conformation. Since there is no accurate crystal structure data on 4,6-*O*-(1-carboxyethylidene)- $\alpha$ -D-galactose, an appropriate model of the bicyclic ring was produced by the fusion of pyruvate to the galactosyl unit following the Arnott and Scott [21] procedure. The pyruvate carboxyl group was affixed in the axial configuration as proposed for the pyruvic acid acetal structures in polysaccharides [22,23].

The function minimized in the least-squares procedure is given by

$$\Omega = \Sigma e_i (\theta_i - \theta_i)^2 + \Sigma w_m (F_m - F_m)^2 + \Sigma k_j (d_j - d_j)^2 + \Sigma \lambda_h G_h$$

$$= \quad E \quad + \quad X \quad + \quad C \quad + \quad L.$$

The first term  $E$  restrains (with weight  $e_i$ ) the conformation or bond angles ( $\theta_i$ )

to preferred domains or to near expected standard values ( ${}_0\theta_i$ ). The best agreement between the observed ( ${}_0F_m$ ) and calculated structure ( $F_m$ ) amplitudes is ensured by the second term  $X$  and  $w_m$  is the weight associated with the  $m$ th observation. The third term  $C$  provides optimization of non-covalent interactions (small  $d_j$ 's driven towards larger  ${}_0d_j$ ), as well as hydrogen bonds (with weight  $k_j$ ), within and between molecules. The  $\lambda_h$  are the Lagrange multipliers and the constraints  $[G_h]$  become zero for a converged model. The 1,3-dioxane pyruvate ring was generated by varying the relevant bond angles and conformation angles while minimizing the function  $\Omega$  with only  $E$ ,  $C$ , and  $L$  terms. In this procedure, the bond angles were tied elastically to standard values, but no explicit restrictions were placed on the values of the conformation angles.

Two dimensional, hard-sphere maps for the two sets of disaccharide units, Glc-Gal and Gal-Glc, were first calculated in order to determine the allowed domains of the glycosidic bridge conformation angles ( $\phi_1, \psi_1$ ) and ( $\phi_2, \psi_2$ ) of the main chain. The center of the allowed region served as the starting set of backbone conformation angles in producing a stereochemically satisfactory molecular model consistent with the observed helix symmetry and pitch.

The two packing parameters,  $\mu$  and  $w$ , respectively, define the orientation and position of a helix in the unit cell. Using the helix as a rigid body, their most probable values were initially ascertained from a two-dimensional survey of the crystallographic  $R$ -value, as well as the contact term  $C$ , in the  $(\mu, w)$  space. After the packing arrangement was set up with these values, the crystal structure was refined by varying a total of 10 conformation angles in the disaccharide unit — 4 in the main chain and 6 rotations defining hydroxymethyl, acetyl and carboxylate groups — along with the two packing parameters. The  $R$  value of this model stabilized at 0.39 corresponding to water-weighted atomic scattering factors [24].

### 3. Development of the crystal structure

Difference Fourier maps having  $(2F_o - F_c)$  as coefficients, in which the  $F_c$ 's were computed using normal atomic scattering factors [25], were synthesized from the polyanion structure to locate cations (Fig. 3) and water molecules, and to verify the orientations of the side chains. The first map revealed several peaks in a region where the carboxylate group on one chain was close to the carboxylate group on the antiparallel chain. A water molecule, as well as a potassium ion, was tried out at each peak and the selection was based on stereochemistry and improved fit with X-ray data. One of the peaks was identified as the potassium ion for which the carboxylate and acetate groups could serve as ligands; and two water molecules were also located in this region. In a subsequent difference map, a third water molecule close to the cation was located, and this led to the completion of an approximately octahedral coordination for the potassium ion. Inclusion of every guest molecule resulted in a 0.02 to 0.03 drop in the  $R$ -value that was a sign for the correctness of the augmented crystal structure. A final difference map at this stage did not show any additional peaks.

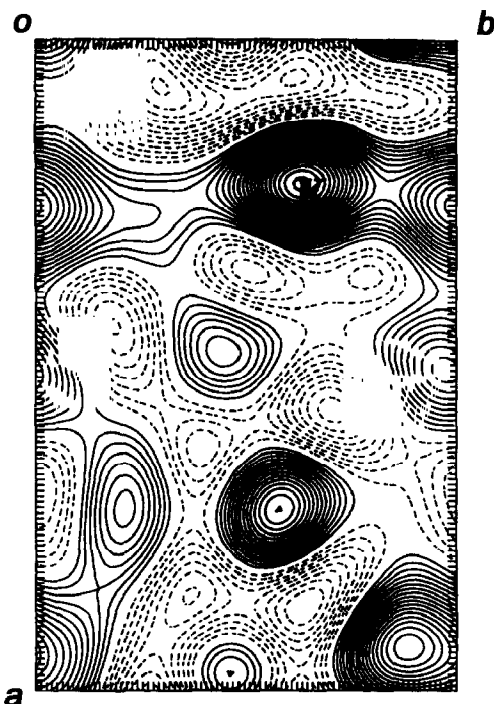


Fig. 3. A section of three-dimensional ( $2F_0 - F_c$ ) map at level  $c/16$ . Positive peaks correspond to the locations of potassium ion (K) and some other atoms (not labeled) of the polysaccharide chain.

Since the inclusion of a potassium ion and three water molecules associated with each disaccharide repeat in the helix accounts for the entire unit cell contents, and is consistent with the measured density of the fiber, further structure analysis was conducted only with normal atomic scattering factors. This included one round of refinement of the positions of the guest atoms and of the polyanion structure with rigid sugar geometry. It was followed by a final round of refinement with flexible sugar rings and relaxed glycosidic bridge bond angles. The shifts for the variables became very small, indicating that the refinement was complete and the  $R$ -value converged to 0.26. The atomic coordinates of the final model, which corresponds to a probable minimum energy state of the polysaccharide and its packing arrangement, are given in Table 1. The observed and calculated structure amplitudes are listed in Table 2.

#### 4. Structural features

**Polyanion conformation.**—The two monosaccharides in the repeating unit are conformationally different across the glycosidic oxygen atoms as much as they are chemically different with regard to the  $\alpha$  and  $\beta$  configurations. Consequently, the polysaccharide chain is sinuous and is a right-handed helix. The substituents

Table 1

Cartesian and cylindrical polar atomic coordinates in a disaccharide repeating unit of the galactoglucan (EPS II)<sup>a</sup>, the associated potassium ion, and three water molecules

Group	Atom	<i>x</i> (Å)	<i>y</i> (Å)	<i>z</i> (Å)	<i>r</i> (Å)	$\phi$ (°)
Glucose	C-1	0.6193	−1.3468	4.9997	1.4824	−65.31
	C-2	0.2776	−0.6721	6.3216	0.7272	−67.56
	C-3	1.5303	−0.4856	7.1639	1.6055	−17.61
	C-4	2.2210	−1.8273	7.3694	2.8761	−39.45
	C-5	2.5088	−2.4254	5.9964	3.4895	−44.03
	C-6	3.1550	−3.7921	6.0783	4.9329	−50.24
	C-7	3.7512	−5.0470	7.9777	6.2884	−53.38
	C-8	3.8433	−4.7420	9.4547	6.1039	−50.98
	O-2	−0.3488	0.5792	6.0628	0.6761	121.05
	O-3	1.1800	0.0945	8.4219	1.1838	4.58
	O-4	3.4430	−1.6531	8.0834	3.8193	−25.65
	O-5	1.2848	−2.5839	5.2624	2.8857	−63.56
	O-6	3.9283	−3.9422	7.2682	5.5653	−45.10
	O-7	3.5449	−6.1397	7.4756	7.0896	−60.00
	H-1	1.2801	−0.6925	4.4122	1.4554	−28.41
	H-2	−0.4466	−1.2902	6.8725	1.3653	−109.09
	H-3	2.2104	0.1903	6.6249	2.2186	4.92
	H-4	1.5652	−2.4923	7.9506	2.9430	−57.87
	H-5	3.1871	−1.7605	5.4415	3.6410	−28.92
	H-61	2.3749	−4.5676	6.0735	5.1481	−62.53
	H-62	3.8200	−3.9358	5.2140	5.4848	−45.86
	H-81	3.6081	−3.6811	9.6256	5.1545	−45.57
	H-82	3.1263	−5.3696	10.0043	6.2134	−59.79
	H-83	4.8627	−4.9532	9.8100	6.9412	−45.53
Galactose	C-1	−2.0436	−1.0801	0.9375	2.3115	−152.14
	C-2	−1.9713	−1.1005	2.4586	2.2577	−150.83
	C-3	−0.5673	−1.4555	2.9235	1.5621	−111.29
	C-4	−0.0858	−2.7309	2.2446	2.7322	−91.80
	C-5	−0.2692	−2.6445	0.7331	2.6582	−95.81
	C-6	0.0464	−3.9397	0.0155	3.9400	−89.33
	C-7	−0.3666	−5.0824	2.1435	5.0956	−94.13
	C-8	1.1078	−5.2820	2.5000	5.3969	−78.15
	C-9	−1.1526	−6.2084	2.6956	6.3145	−100.52
	O-2	−2.3638	0.1699	2.9653	2.3699	175.89
	O-3	−0.5654	−1.6472	4.3396	1.7415	−108.94
	O-4	−0.8225	−3.8556	2.7198	3.9423	−102.04
	O-5	−1.6373	−2.3463	0.4144	2.8611	−124.91
	O-6	−0.5330	−5.0346	0.7240	5.0627	−96.04
	O-81	1.7414	−6.1328	1.8387	6.3752	−74.15
	O-82	1.5680	−4.5792	3.4256	4.8402	−71.10
	H-1	−3.0778	−0.8698	0.6272	3.1984	−164.22
	H-2	−2.6846	−1.8410	2.8498	3.2552	−145.56
	H-3	0.1023	−0.6218	2.6653	0.6302	−80.66
	H-4	0.9796	−2.8867	2.4699	3.0484	−71.26
	H-5	0.4000	−1.8723	0.3259	1.9145	−77.94
	H-61	1.1371	−4.0612	−0.0595	4.2174	−74.36
	H-62	−0.3435	−3.8942	−1.0121	3.9093	−95.04
	H-91	−0.4757	−6.9202	3.1908	6.9365	−93.93
	H-92	−1.8788	−5.8249	3.4274	6.1204	−107.88
	H-93	−1.6887	−6.7162	1.8803	6.9252	−104.11



Table 1 (continued)

Group	Ato	$x$ (Å)	$y$ (Å)	$z$ (Å)	$r$ (Å)	$\phi$ (°)
Ion	K	3.0799	−3.5921	1.0925	4.7317	−49.39
Water	W1	3.0838	−6.8288	4.6771	7.4928	−65.70
	W2	−0.4347	−4.5064	5.6035	4.5273	−95.51
	W3	−2.8120	2.3931	5.7958	3.6924	139.60

<sup>a</sup> The coordinates of atoms in the two repeating units in one turn of helix I at the corner of the unit cell are  $\{x, y, z\}$  and  $\{-x, -y, (c/2) + z\}$ , respectively. Those of helix II at the center of the unit cell are  $\{(a/2) + x, (b/2) - y, -z\}$  and  $\{(a/2) - x, (b/2) + y, (c/2) - z\}$ .

Table 2

Observed and calculated structure amplitudes <sup>a</sup> for the potassium salt of galactoglucan

$h$	$k$	$l = 0$	1	2	3	4	5	6				
0	0	M [1124]	N [0]	M [136]	N [0]	M [60]	N [0]	M [116]				
1	0	N [0]	(24) (44)	78 118	30 72	61 12	168 107	122 129				
0	1	N [0]	130 90	47 167	(39) (45)	(44) (54)						
1	1	141 9	210 271	(41) (158)								
2	0	(44) (102)	226 205	171 190					84 62	97 99	192 153	237 178
2	1	[54] [25]	123 173	116 166					119 86	131 83	[75] [33]	[87] [37]
0	2	(68) (103)	135 157	151 65								
3	0	(68) (109)	(67) (72)	[69] [35]					164 161	(110) (137)	177 133	
3	1	(75) (75)	253 237	191 202	(80) (112)							
2	2	123 140	141 134	158 131	103 101							
4	0	243 217	172 125	124 106	151 156							
3	2	170 152	133 142	165 217								
0	3	131 69	125 127	129 103	136 137							
1	3	[123] [64]	[120] [60]									
4	2								151 155	(225) (277)		
5	0								(136) (150)			
5	1											

<sup>a</sup> In each reflection box, the observed amplitude is given in the first line and the calculated amplitude (italics) in the second line. The curved and rectangular brackets refer respectively to below threshold reflections included in, and rejected from, the least-squares refinement. M denotes meridional reflection and N systematically absent reflection, respectively. The calculated structure amplitudes include a temperature factor with  $B = 4.0 \text{ Å}^2$ .

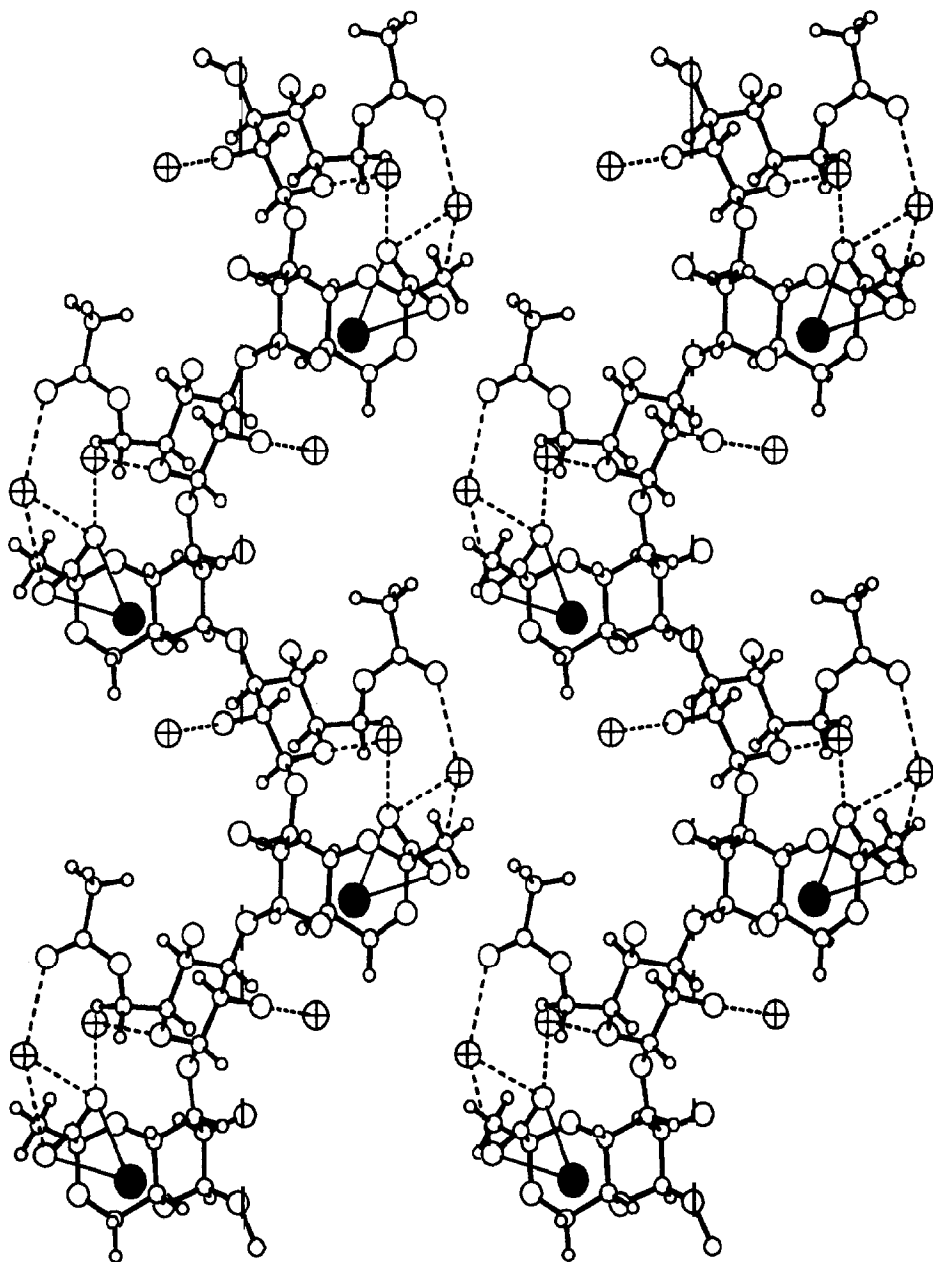


Fig. 4. A stereoscopic side view of two turns of the right-handed galactoglucan helix stabilized by the potassium ions (filled circle) and water molecules (crossed circle). Dashed lines denote hydrogen bonds. Thin lines connect each potassium ion to two of its ligands. The vertical bar on the right measures the helix pitch.

(acetate and pyruvate) occur on the periphery such that the acetate oxygen atom O-7A ( $r = 7.0 \text{ \AA}$ ) is farthest from the helix axis. A side view of the helix shown in Fig. 4 highlights these observations.

The local turn angles, measured as the difference in cylindrical polar angle  $\phi$  (Table 1) of adjacent bridge oxygen atoms, are  $113.5$  and  $66.5^\circ$  along residues A and B, respectively, indicating that the twist measured across the glucosyl unit is nearly twice that across the galactosyl unit. The corresponding projected lengths of these residues along the helix-axis are  $4.1$  and  $3.9 \text{ \AA}$  and their bridge oxygen atoms are in the interior of the helix at  $r = 1.2$  and  $1.7 \text{ \AA}$ . Considering the fact that the respective O-1 to O-3 virtual bond distances are  $4.8$  and  $4.2 \text{ \AA}$ , the EPS II helix is fairly extended.

The major conformation angles ( $\phi$ ,  $\psi$ ,  $\theta$ , and  $\chi$ ) in the helix are listed in Table 3. There is generally good agreement between these values and those predicted for the isolated chain from the conformational energy surface calculations [15]. In terms of molecular morphology, it is important to note that there are no direct intrachain hydrogen bonds across either glycosidic bridge oxygen atom in the EPS II helix. In this regard, two other  $(1 \rightarrow 3)$ -linked polymers consisting of simple monosaccharide repeating units, namely, a  $\beta$ -D-xylan [26,27] and the  $\beta$ -D-glucan known as curdlan [28] are similar examples; and the polysaccharide chains in both polymers are reported to be fairly flexible in solution. The stability of the EPS II helix is, apparently, derived from water molecules *W1* and *W2* which connect adjacent units A and B which are on the nonreducing and reducing side, respectively. *W1* hydrogen bonds with O-7A, O-81B, and O-82B; *W2* with O-5A and O-82B (Fig. 4). However, there is no such water bridge between adjacent A and B units which are on the reducing and nonreducing side, respectively. This suggests that the main chain is still flexible around this region.

The quite different orientations of the galactosyl and glucosyl units in the helix may be visualized in Fig. 4. While counting the saccharide units upwards from the bottom, units 1 and 2 are on the same side, but 2 and 3 are on opposite sides, of the helix axis. This behavior mirrors the previously mentioned differences in  $\phi$  values between successive O-3A and O-3B atoms (Table 1) which are in the interior of the helix. This effect is further magnified if the peripheral atoms O-7A

Table 3

Major conformation angles (and esd) in the final model of the galactoglucan helix

Conformation angle ( $^\circ$ )	Galactoglucan	Remarks
$\phi_1(\text{O-5B-C-1B-O-3A-C-3A})$	88(1)	$\alpha$ -(1 $\rightarrow$ 3)
$\psi_1(\text{C-1B-O-3A-C-3A-C-4A})$	100(1)	$\alpha$ -(1 $\rightarrow$ 3)
$\chi_1(\text{C-4A-C-5A-C-6A-O-6A})$	-29(2)	hydroxymethyl
$\theta_1(\text{C-5A-C-6A-O-6A-C-7A})$	132(3)	acetyl
$\theta_2(\text{C-6A-O-6A-C-7A-C-8A})$	-143(3)	acetyl
$\theta_3(\text{O-6A-C-7A-C-8A-H-81A})$	24(4)	acetyl
$\phi_2(\text{O-5A-C-1A-O-3B-C-3B})$	-101(1)	$\beta$ -(1 $\rightarrow$ 3)
$\psi_2(\text{C-1A-O-3B-C-3B-C-4B})$	88(2)	$\beta$ -(1 $\rightarrow$ 3)
$\theta_4(\text{O-6B-C-7B-C-8B-O-81B})$	-44(3)	pyruvate
$\theta_5(\text{O-6B-C-7B-C-9B-H-91B})$	119(2)	pyruvate

Table 4

Attractive interactions involving the polyanion, potassium ion, and water molecules responsible for the association of the galactoglucan helices <sup>a</sup>

Interaction	Atom X	Atom Y	X···Y (Å)	Precursor P	P–X···Y (°)
Interchain	O-4A	O-81B(II)	2.88	C-4A	107
Potassium coordination	O-81B	K	2.97	C-8B	77
	O-82B	K	2.95	C-8B	78
	O-7A(II)	K	2.51	C-7A	154
	O-4A(II, 110)	K	3.28	C-4A	96
	O-5B(II, 110)	K	3.12	C-5B	161
	W1(II)	K	2.94		
Water bridges					
Intrachain	O-7A	W1	2.92	C-7A	129
	O-81B	W1	3.21	C-8B	84
	O-82B	W1	2.98	C-8B	94
	O-5A	W2	2.60	C-5A	125
	O-82B	W2	2.96	C-8B	108
	O-2A	W3	3.07	C-2A	153
Interchain	O-7A(II)	W3	2.99	C-7A	86

<sup>a</sup> All atoms belong to helix I at the corner, except those labeled by II in parentheses which refers to helix II at the center, of the unit cell. 110 in parentheses denotes unit cell translation along the *a*- and *b*-axis, respectively.

and O-81B are considered for reference;  $\Delta\phi$  is 14° for O-7A–O-81B, but is almost 166° for O-81B–O-7A, while progressing along the chain. Thus, the helix effectively uses the Gal-Glc linkage for most of the helical twist (180°).

**Intermolecular association.**—Table 4 lists the attractive interactions among the EPS II helix, potassium ions, and water molecules which are responsible for the associative properties of the polymer chains. Consistent with standard deviations (up to 4°) for conformation angles (Table 3), estimated standard deviations for hydrogen bond distances (Table 4) are  $\sim 0.1$  Å. Water molecules *W1* and *W2* participate exclusively in intrachain interactions so as to connect the carboxylate group of the pyruvated galactosyl unit with the acetate group of the acetylated glucosyl unit. On the other hand, *W3* spans a pair of helices in the unit cell. Each potassium ion, located near a carboxylate group, interacts with three polysaccharide chains and a water molecule (Fig. 5). The coordination shell of the ion consists of six ligands which constitute a distorted octahedron: atoms O-81B and O-82B of helix II, O-4A and O-5B of helix I, and *W1* and O-7A of helix I(100) for the potassium ion marked by an arrow in Fig. 5. This region reveals that atom O-7A is crucial for the stability of the three-dimensional structure via water bridges involving *W1* and *W3*. *W1* interacts with not only K<sup>+</sup>, but also with the oxygen atoms in the pyruvate and acetate groups, as already mentioned. *W3* forms a hydrogen bond with atom O-2A of helix II. The network of hydrogen bonds mediated by pyruvate and *W1* leads to a series of  $\cdots \text{COO}^- \cdots \text{K}^+ \cdots \text{W} \cdots \text{COO}^- \cdots$  interactions. While *W1* has the key role of bridging pyruvate and

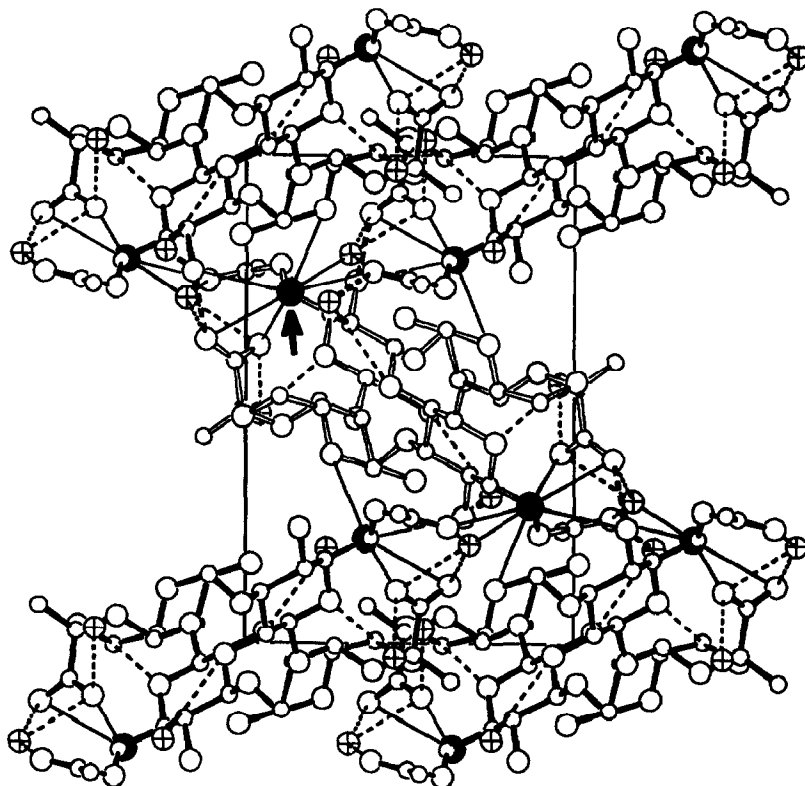


Fig. 5. Packing arrangement, as viewed down the *c*-axis, of four galactoglucan molecules at the corners and an antiparallel molecule at the center of the unit cell. Thin and thick dashed lines denote intra- and inter-chain hydrogen bonds, respectively. Potassium ions (filled circle) are connected to their ligands by thin lines. Association of helices is facilitated by ions, water molecules (crossed circle), and peripheral pyruvic and acetyl groups belonging to neighboring polysaccharide chains.

acetate groups (Fig. 4) within the chain,  $K^+$  plays a similar role (Fig. 5) between the chains.

The packing arrangement reveals that helices at adjacent corners of the unit cell have the same polarity and are too far apart to encounter any close contacts between them. However, the helices at the corner and center of the unit cell are antiparallel to each other, almost 9.0 Å apart (Figs. 5 and 6), and yet make the one and only direct interchain hydrogen bond in every repeating unit, connecting the interior of one helix with the periphery of the other; this involves atoms O-4A of helix I and O-81B of helix II. In addition, the potassium ion and the water molecule *W1* connect up to three polysaccharide chains (Table 4). As a result, there is a continuous connectivity, in a zigzag fashion, between up and down helices along the diagonal of the unit cell in the *c*-axis projection (Fig. 5). This arrangement, stabilized by the network of hydrogen bonds and ionic interactions, both of which are facilitated by water molecules, is fairly tight.

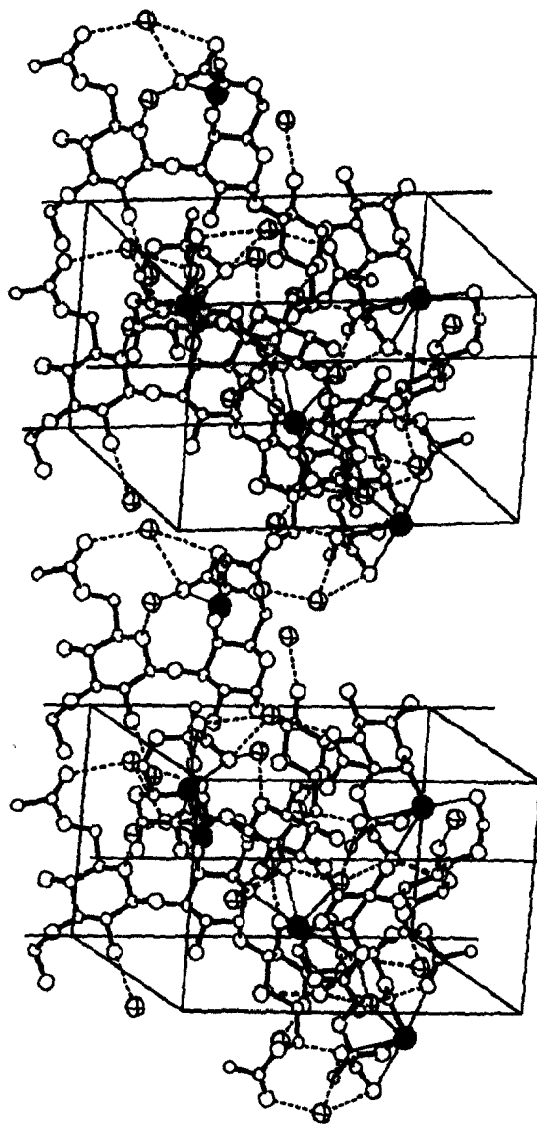


Fig. 6. A stereoscopic view of the unit cell contents showing three helices — two in filled bonds and one of opposite polarity in open bonds — connected and stabilized by  $\cdots \text{COO}^- \cdots \text{K}^+ \cdots \text{W} \cdots \text{COO}^- \cdots$  interactions.

## 5. Discussion

The ability of EPS II, the simple and linear acidic exopolysaccharide with a disaccharide repeating unit, to act as a potent substitute for EPS I, which has an octasaccharide repeating unit, in invasion and nodule development of *Medicago sativa* is quite striking [16,29], given the very considerable differences in chemical sequences between the two. For example, in every repeating unit, EPS I contains succinyl modifications, but EPS II does not; the sugar composition of EPS I is quite different from that of EPS II; EPS I has a side chain, but EPS II does not; EPS I has only  $\beta$ -linkages, whereas EPS II has both  $\alpha$ - and  $\beta$ -linkages; and the 1-carboxyethylidene (pyruvate) modification is on the D-glucosyl unit in the case of EPS I, but on the D-galactosyl unit in EPS II. However, there are observations to suggest [6,17] that specific structural features of exopolysaccharides are important for at least one role, namely participating in the recognition of root hairs in symbiosis, and that the identity of the host determines which structural features of an acidic exopolysaccharide are important for this role.

The only common feature found in the backbone of both polysaccharides is the  $\beta$ -D-glucosyl-(1  $\rightarrow$  3)-D-galactosyl linkage. While each sugar unit in this linkage is modified in EPS II, it is not in EPS I, but in the latter, the positions of acetyl and succinyl substituents have not yet been assigned [3]. If the D-glucosyl units of EPS I were to carry a 6-O-acetyl substituent and the galactosyl unit a succinyl modification, then each polysaccharide would contain the common structural feature in its backbone of an 6-O-acetyl-D-glucosyl unit joined by a  $\beta$ -(1  $\rightarrow$  3) linkage to a D-galactosyl unit carrying an acidic modification. It has been shown that a crude enzyme preparation which cleaves EPS II at the  $\beta$ -D-glucosyl-(1  $\rightarrow$  3)- $\alpha$ -D-galactosyl linkage, also cleaves EPS I at this position [30]. The presence of such a putative common structural feature could account for how two structurally diverse exopolysaccharides can substitute for each other in a process that seems to have a requirement for specific structural features. This finding might provide the clue that one of the functions of the exopolysaccharides is to help the bacteria avoid plant defense responses. This suggestion is based on a report that  $\beta$ -D-(1  $\rightarrow$  3)-glucanases are involved in plant defense responses to pathogens [31].

Results from this X-ray diffraction study show that the EPS II molecule forms a two-fold helix of pitch 15.89 Å and two helices are packed in the unit cell corresponding to space group P2<sub>1</sub>2<sub>1</sub>2<sub>1</sub>. The up and down pointing helices, at the corners and center of the unit cell, respectively, communicate via a series of  $\cdots \text{COO}^- \cdots \text{K}^+ \cdots \text{W} \cdots \text{COO}^- \cdots$  interactions which are further stabilized by the acetyl groups and water molecules (Table 4, Figs. 5 and 6). This implies that both pyruvate and acetyl groups are essential for the stability and association of the polysaccharide chains. Consequently, these substituents are equally important to facilitate intimate contacts between the polysaccharide and the root hairs of leguminous plants in the infection process.

Solution properties [14,15] indicate that the conformation of EPS II is not ordered in dilute solution over a wide range of temperature. This is in accordance with the fact that the polymer chain itself is somewhat flexible since there are no

hydrogen bonds within the main chain atoms. The close interresidue encounters among the backbone oxygen atoms — O-4A–O-2B (3.4 Å) and O-2B–O-2A (3.8 Å) — are too large to be reckoned as hydrogen bonds. A comparison with the chain dimensions of a (1 → 3)- $\alpha$ -D-galactan [14,15] has led to the suggestion that EPS II has a more rigid random-coil conformation. The three-dimensional structure of the galactoglucan described above demonstrates that this flexibility would be disciplined by the water bridge O-82B  $\cdots$  W1  $\cdots$  O-5A in every repeating unit. Hence, it is believed that the molecular structure and organization of the local stiff region of EPS II in solution would be closely related to that of EPS II elucidated in fibers.

### Acknowledgments

This work was supported by the Industrial Consortium of the Whistler Center of Carbohydrate Research, the National Science Foundation (MCB-9219736), and the Purdue Research Foundation.

### References

- [1] C.L. Diaz, L.S. Melchers, P.J.J. Hooykaas, B.J.J. Lugtenberg, and J.W. Kijne, *Nature (London)*, 338 (1989) 579–581.
- [2] J.A. Downie and A.W.B. Johnston, *Cell*, 47 (1986) 153–154.
- [3] P. Åman, L.-E. Franzén, J.E. Darvill, M. McNeil, A.G. Darvill, and P. Albersheim, *Carbohydr. Res.*, 103 (1982) 77–100.
- [4] A. Heyraud, M. Rinaudo, and B. Courtois, *Int. J. Biol. Macromol.*, 8 (1986) 85–88.
- [5] J.D. Linton, M. Evans, D.S. Jones, and D.N. Gouldney, *J. Gen. Microbiol.*, 133 (1987) 2961–2969.
- [6] J.A. Leigh, E.R. Signer, and G.C. Walker, *Proc. Natl. Acad. Sci. U.S.A.*, 82 (1985) 6231–6235.
- [7] J.A. Leigh, J.W. Reed, J.F. Hanks, A.M. Hirsch, and G.C. Walker, *Cell*, 51 (1987) 579–587.
- [8] P. Åman, M. McNeil, L.-E. Franzén, A.G. Darvill, and P. Albersheim, *Carbohydr. Res.*, 95 (1981) 263–282.
- [9] M. Dentini, V. Crescenzi, M. Fidanza, and T. Coviello, *Macromolecules*, 22 (1989) 954–959.
- [10] G. Grayvanis, M. Milas, M. Rinaudo, and A.J. Clarke-Sturman, *Int. J. Biol. Macromol.*, 12 (1990) 195–200.
- [11] L.P.T.M. Zevenhuizen, in E.A. Dawes (Ed.), *Novel Biodegradable Microbial Polymers*, Kluwer Academic, The Netherlands, 1990, pp 387–402.
- [12] L.P.T.M. Zevenhuizen, in V. Crescenzi, I.C.M. Dea, S. Paoletti, S.S. Stivala, and I.W. Sutherland (Eds.), *Biomedical and Biotechnological Advances in Industrial Polysaccharides*, Gordon and Breach, New York, 1989, pp 301–311.
- [13] L.P.T.M. Zevenhuizen and P. Faleschini, *Carbohydr. Res.*, 209 (1991) 203–209.
- [14] L. Navarini, A. Cesàro, and S.B. Ross-Murphy, *Carbohydr. Res.*, 223 (1992) 227–234.
- [15] A. Cesàro, G. Tomasi, A. Gamini, S. Vidotto, and L. Navarini, *Carbohydr. Res.*, 231 (1992) 117–135.
- [16] J. Glazebrook, J.W. Reed, T.L. Reuber, and G.C. Walker, *Int. J. Biol. Macromol.*, 12 (1990) 67–70.
- [17] S. Long, J.W. Reed, J.W. Himawan, and G.C. Walker, *J. Bacteriol.*, 170 (1988) 4239–4248.
- [18] R.P. Millane and S. Arnott, *J. Appl. Crystallogr.*, 18 (1985) 419–423.
- [19] R.P. Millane and S. Arnott, *J. Macromol. Sci. Phys.*, 24 (1985) 193–227.
- [20] P.J.C. Smith and S. Arnott, *Acta Crystallogr. Sect. A*, 34 (1978) 3–11.



- [21] S. Arnott and W.E. Scott, *J. Chem. Soc., Perkin Trans. 2*, (1972) 324–335.
- [22] P.A.J. Gorin, M. Mazurek, H.S. Duarte, M. Iacomini, and J.H. Duarte, *Carbohydr. Res.*, 100 (1982) 1–15.
- [23] P.J. Garegg, P.-E. Jansson, B. Lindberg, F. Lindh, J. Lönngren, I. Kvarnström, and W. Nimmich, *Carbohydr. Res.*, 78 (1980) 127–132.
- [24] S. Arnott, R. Chandrasekaran, A.W. Day, L.C. Puigjaner, and L.M. Watts, *J. Mol. Biol.*, 149 (1981) 489–505.
- [25] International Tables For X-ray Crystallography, Vol. IV, Kynoch Press, England 1974, pp 99–101.
- [26] E.D.T. Atkins and K.D. Parker, *J. Polym. Sci.*, C28 (1969) 69–81.
- [27] E.D.T. Atkins, K.D. Parker, and R.D. Preston, *Proc. Roy. Soc. London, Ser. B*, 173 (1969) 209–221.
- [28] W.S. Fulton and E.D.T. Atkins, *ACS Symp. Ser.*, 141 (1980) 385–410.
- [29] H. Zhan, S.B. Levery, C.C. Lee, and J.A. Leigh, *Proc. Natl. Acad. Sci. U.S.A.*, 86 (1989) 3055–3059.
- [30] J. Glazebrook and G.C. Walker, *Cell*, 56 (1989) 661–672.
- [31] E. Kombrink, M. Schroeder, and K. Hahlbrock, *Proc. Natl. Acad. Sci. U.S.A.*, 85 (1988) 782–786.